공학석사학위논문

Magnetic Nanoparticles Embedded Silver Nanoshell as Highly Sensitive SERS Probe

자성나노입자를 포함한 은 나노쉘의 합성과 민감한 표면증강 라만산란 프로브로서의 응용

2017년 8월

서울대학교 대학원

화학생물공학부

박 소 연

Magnetic Nanoparticles Embedded Silver Nanoshell as Highly Sensitive SERS Probe

자성나노입자를 포함한 은 나노쉘의 합성과
민감한 표면증강 라만산란 프로브로서의 응용

지도 교수 이 윤 식

이 논문을 공학석사학위논문으로 제출함.

2017년 8월

서울대학교 대학원
화학생물공학부
박 소 연

박소연의 공학석사학위논문을 인준함.
2017년 6월

위 원 장 장 정 식 (인)

부위원장 이 윤 식 (인)

위 원 김 대 형 (인)

ABSTRACT

Magnetic Nanoparticles Embedded Silver Nanoshell as Highly Sensitive SERS Probe

자성나노입자를 포함한 은 나노쉘의 합성과
민감한 표면증강 라만산란 프로브로서의 응용

So Yeon Park

School of Chemical and Biological Engineering

The Graduate School

Seoul National University

SERS (Surface-enhanced Raman scattering) is an efficient tool for multiplexed analysis of various targets because it has unique signal patterns with narrow band width and is stable to photo-bleaching. The structure of metal substrate is very important in obtaining strong SERS signals. So far, various approaches have been tried to develop new types of metal substrate for sensitive detection of targets at low concentration. In this thesis, a new type of SERS nanoprobe was synthesized which has hundreds of iron oxide magnetic nanoparticles at the core part, and silver shell at the outer part. (Magnetic silver

Nanoshell, M AgNS) The surface of silver shell has bumpy structure, which could lead to the formation of 'hot spots', affording strong SERS signal. Besides, SERS signal could be further intensified by magnetic-induced aggregation. Through this M AgNS nanoprobe, 4-fluorothiophenol (4-FBT) was detected at low concentration as 1 μM, which corresponds to 16 ppb. Thiram and malathion, which are mainly used pesticides in the farm, were also detected at low concentrations using the aggregated M AgNS. The limit of detection (LOD) for thiram was 10 μM, which corresponds to 3 ppm. M AgNS nanoprobe is expected to be utilized in on-site detection of various analytes at low concentrations using a 785 nm portable Raman system.

Keywords**:** Surface enhanced Raman scattering, silver nanoshell, magnetic induced aggregation, molecular detection,

Student number: 2015-21063

TABLE OF CONTENTS

LIST OF TABLES

LIST OF FIGURES

LIST OF ABBREVIATIONS

SERS	Surface-enhanced Raman scattering
EM	Electromagnetic
M AgNS	Magnetic Ag nanoshell
M silica NP	Magnetic silica nanoparticle
NP	Nanoparticle
NIR	Near-infrared
UV	Ultraviolet
EtOH	Ethanol
TEOS	Tetraethylorthosilicate
MPTS	3-mercaptopropyltrimethoxysilane
EG	Ethylene glycol
PVP	Poly(vinyl pyrrolidone)
4-FBT	4-Fluorothiophenol
TEM	Transmission electron microscope
SEM	Scattering electron microscope
APTS	3-Aminopropyltriethoxysilane
DMF	*N,N*-Dimethylformamide
Vis	Visible

I. Introduction

I. 1 The Advantages of SERS

Raman scattering is a vibrational spectroscopy which is related to the molecular structure. Since the Raman signal has a very narrow band width, the Raman spectrum can be direct used for specific identification. However, Raman signals are very weak. As a result, signal enhancement is necessary to use this Raman scattering technique for the detection of molecules in a low concentration.[1] Surface enhanced Raman spectroscopy (SERS) was first observed as strong Raman signals of pyridine adsorbed on roughened silver surfaces in 1974. The Raman intensities could be amplified several orders of magnitude on a metallic surface and these amplified intensities were due to electromagnetic (EM) field enhancement.[2] The SERS effect occurs when the analytes are located at or very close to coinage-metal (Ex. Au, Ag and Cu) nanostructures. As shown in Figure 1.1, when the incident light reaches the metal-nanomaterial's surface, free electrons of metal can be excited and oscillated because the size of nanomaterial is smaller than the wavelength of light. According to the progression of EM field,

free electrons move with pulled back and forth between the negatively charged electrons and the positive nuclei and this formulates the electron cloud with collective oscillation. This collective oscillation is referred to as surface plasmon and localized surface plasmons (LSPs) which occur around the surface of metal-nanomaterial. This can enhance the local EM field intensity by several orders of magnitude. [1, 3] Through this mechanism, SERS can offer strongly enhanced signals by a factor of 10^{10}-10^{15} compared to normal Raman scattering.[1]

SERS offer several distinct advantages compared with other methods for target imaging and detection. Compared to fluorescence, SERS have high sensitivity[4], and the signals are much more stable against photobleaching. In addition, as shown in Figure 1.2, the peak width of Raman signals is about 1-2nm which is 10-100 times narrower than that of fluorescence emission from organic dyes or quantum dots.[1] Furthermore, SERS has other advantages such as multiplex capacity[1] and non-disturbance from water.[5] Therefore, SERS technique can be utilized in various fields such as molecular detection[6], diagnosis[7] and bio-imaging.[8]

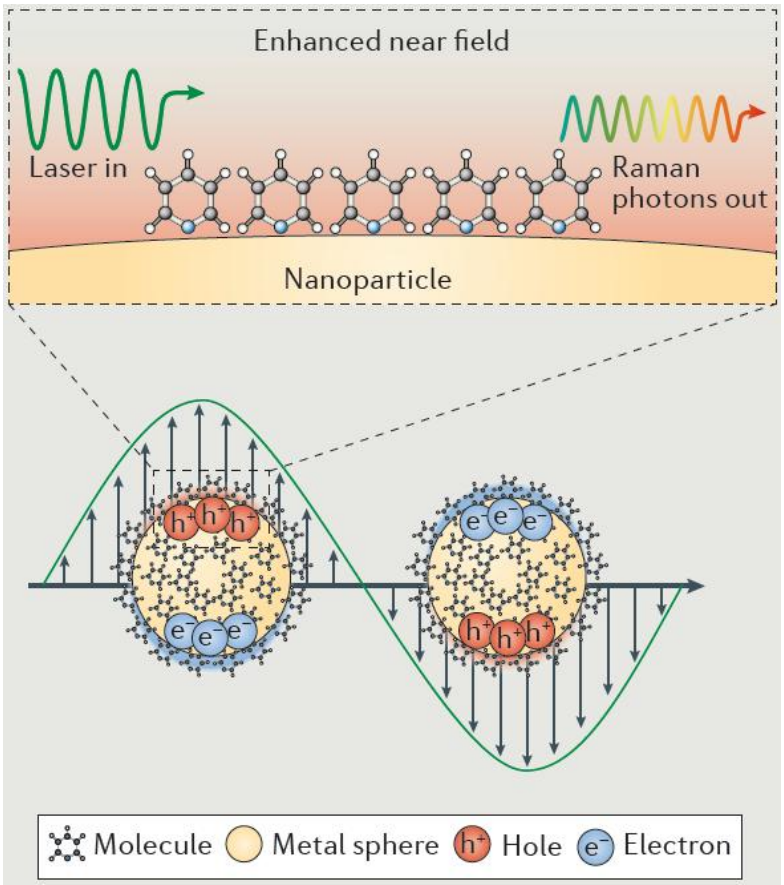

Figure 1.1 Schematic representation of the localized surface plasmon resonance mechanism of SERS.[9]

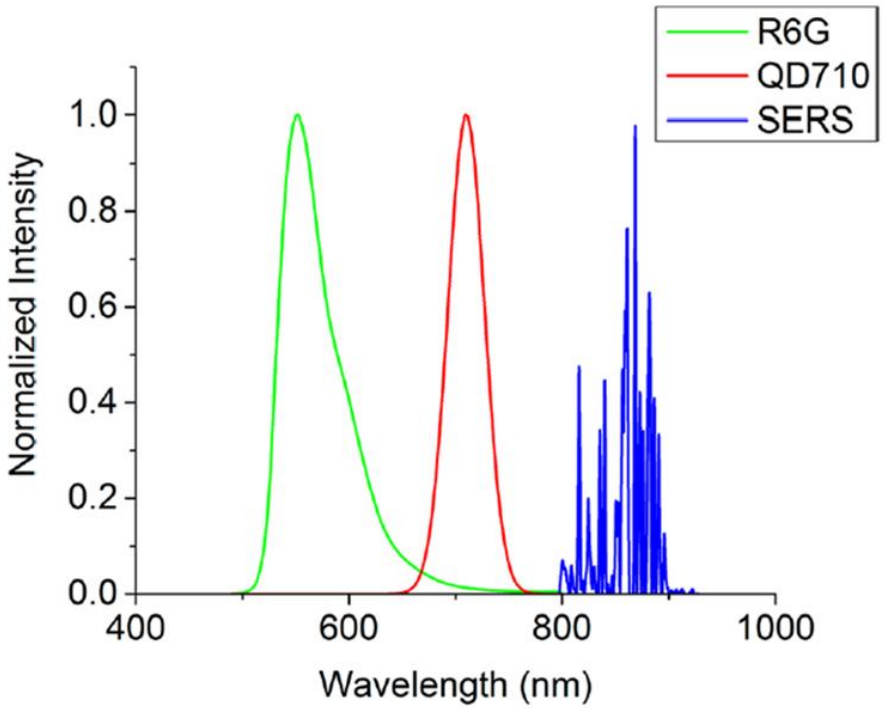

Figure 1.2 Comparison of the spectral characteristics of SERS, quantum dots (QD, emitting at 710nm), and Rhodamine 6G (R6G).[1]

I. 2 The importance of 'Hot Spot' for SERS signal enhancement

For the last decades, a great effort has been made to enhance the SERS signals. Various kinds of nanomaterials have been developed to induce the 'hot spot' phenomenon. The 'hot spot' is localized region of highly concentrated electromagnetic field to give the enhanced Raman signal.[9] The 'hot spot' is generated by two factors.

The First one is related to the shape of nanomaterials. The strong EM field can be formed at the sharp corners or intra-particle gaps. From these reasons, noble nano-metals such as silver and gold NPs have been prepared in very diverse shapes, including nanoshells[10], nanospheres[11], nanorods[12], nanoprism[13], nanostars[14], nanowires[15], nanocubes[16] and other shapes. Previously, silver nanoshell has been developed in my laboratory. It is known that solid silver has a stronger and sharper EM field than solid gold. In addition, compared to nanospheres, nanoshells could give benefits for detection of target molecules because it could form the 'hot spots' between nano-gaps in silver shell, producing the stronger EM field. As a result, silver nanoshell could induce strong enhanced Raman signals because of its bumpy shape.[10]

The second one is related to the close proximity among single nanostructures. 'Hot spot' can be created within crevices or gaps between two or more NPs either in an aggregated state or in close proximity to each other.[9] As shown in Figure 1.3, the SERS enhancement depends on the gap size. When the gap size between the Au nanosphere dimer is reduced from 10 to 2 nm, the SERS enhancement increases. Considering this factor, silver embedded magnetic NPs (Ag-M-dots) were also developed in my laboratory. As shown in Figure 1.4.a, Ag-M-dots were aggregated to create crevice structures between the nanoparticles under the application of an external magnet. Aggregation of NPs by a magnet could produce the 'hot spot' and led to the enhanced Raman signals for detection of adenine at a low concentration.[1] On the other hand, 'dry state method' for SERS enhancement was also reported. As shown in Figure 1.4b, there are four different states of agglomerates from the wet state to the dry state. At first, the particles are completely surrounded by liquid. As the evaporation is proceeded, the liquid- phase content decreased and the inter-particle gap becomes smaller. Through the inter-particle gap, a number of 'hot spots' are formed by drying aggregation, and this can

give advantages to improve the sensitivity of SERS, compared to the solution-based detection.[17]

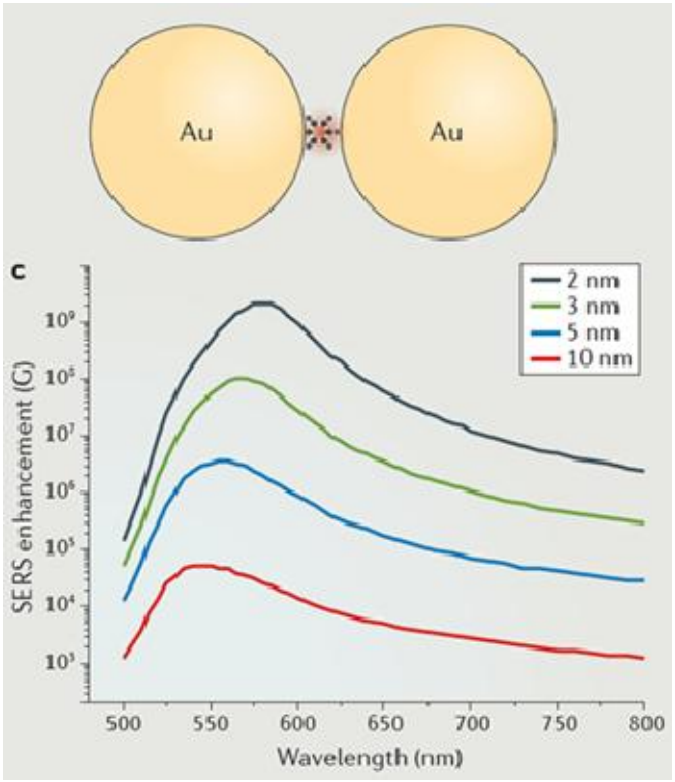

Figure 1.3 SERS enhancement according to the gap size between Au nanoparticles.[9]

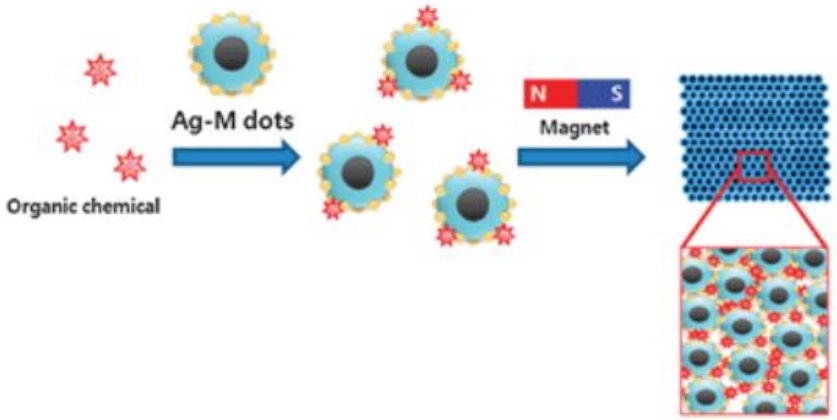

Figure 1.4.a Illustration of magnetic field induced aggregation of Ag-M-dots.[2]

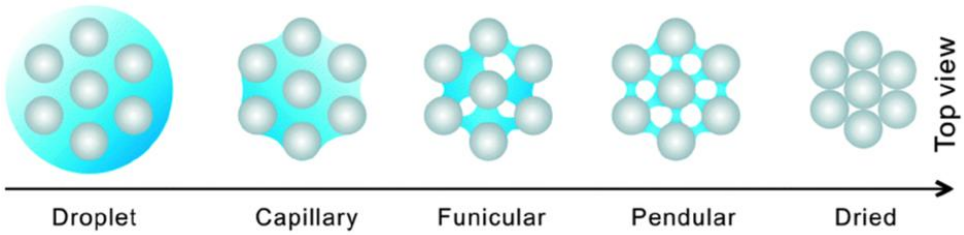

Figure 1.4.b Illustration of agglomerates state of NPs from wet to dry states.[18]

I. 3 SERS technique for molecular detection

Recently, SERS technique is considered as one of the most promising analytical tools due to its special properties. First, high sensitivity of SERS enables to detect the analytes in low concentrations, even at a single molecule level. Second, SERS spectra are closely related to the chemical structure, affording fingerprint like information. Third, SERS is a fast analytical technique, so it enables the rapid detection of analyte. Fourth, since water is a weak Raman scatterer, SERS techniques can be directly applied in water without disturbance from background signals. Fifth, both chemical and biological molecules can be detected by SERS technique. Most of the techniques such as chromatography, electrochemical methods require the sophisticated instruments and complex sampling processes, which can limit the broad application. On the other hand, SERS technique is cost-effective process because miniaturized spectrometers such as portable Raman spectrometer are now available. These outstanding advantages have led to the considerable improvements of SERS-based molecular detection. In recent years, SERS technique becomes more attractive and many achievements have been reported in environmental analysis field. For

example, detection of pollutants such as organic pollutants[10], heavy metal ions[19], pathogens[20] have been developed actively.

I. 4 Research Objectives

In this thesis, a new type of SERS nanoprobe having Fe_3O_4 NPs at the core part and bumpy shaped silver shell at the outer part was fabricated using as a template silica NP. This SERS nanoprobe is named as M AgNS, exhibited highly enhanced Raman signal by the mechanism, which were presented at the previous introduction part. In addition, we demonstrate the potential of M AgNS in sensitive detection of molecules at a low concentration using a portable Raman spectrometer.

II. Experimental Section

II. 1. Chemicals and Materials

Tetraethylorthosilicate (TEOS), 3-aminopropyltriethyoxysilane (APTS), caffeic acid, polyvinylpyrrolidone (PVP, MW=10000 or 40000), 3-mercaptopropyl trimethoxysilane (MPTS), ethylene glycol (EG), 4-chlorobenzenethiol (4-FBT), silver nitrate ($AgNO_3$, 99.99 %) and malathion were purchased from Sigma-Aldrich Inc (USA). Ammonium hydroxide (NH4OH, 30 %), absolute ethanol (99.5 %), ethanol (98 %), *N,N*-dimethylformamide (DMF), *N,N*-diisopropylethylamine (DIEA), methylene chloride (MC), diethyl ether and isopropyl alcohol (IPA) were provided by Daejung chemical (Gyeong-gi, Korea). Fe_3O_4 nanoparticles (NP) were purchased from Ocean Nanotech (USA). HBTU and HOBT were purchased from Bead Tech. Tetramethylthiuram disulfide (thiram, 97 %) was purchased from Alfar Aesar (USA).

II. 2 Instruments

The morphology and the size of NPs were characterized using transmission electron microscope (TEM, LIBRA 120, Carl Zeiss) and field emission scanning electron microscope (FE- SEM, JSM-6701F, JEOL). Absorption spectra of M AgNSs and M silica NPs were measured using a UV/Vis spectrometer (Optizen 2120UV, Mecasys). The SERS spectra were obtained with a portable-Raman system (B&W TEK, i-Raman) which is equipped with a diode laser emitting at 785 nm. Hysteresis loop of M AgNSs was measured using a physical property measurement system (PPMS-14, Quantum Design).

II. 3 Preparation of catechol-functionalized silica NPs

Silica NPs (250 nm) were synthesized by Stöber method. Tetraorthosilicate (TEOS) (1.6 mL) was added to 40 mL of absolute ethanol and 4.0 mL ammonium hydroxide (30% in water) was added to the TEOS solution. This mixture was stirred (160 rpm) for 18 h at room temperature. The resulting silica NPs were centrifuged (8500 rpm, 15 min) and washed with absolute ethanol several times. To obtain amine functional groups on the surface of silica NPs, 40 mg of silica NPs were dispersed in 20 mL of absolute ethanol. After 200 μL of H_2O, 100 μL of APTS and 100 μL of ammonium hydroxide were added, the mixture was stirred in a shaking incubator (160 rpm) for 18 h at room temperature. The resulting amine-functionalized silica NPs were centrifuged (8500 rpm, 15 min) and washed with absolute ethanol and DMF for several times. To introduce catechol functional groups to the silica NPs, 20 mg of amine-functionalized silica NPs were dispersed in 5 mL of DMF. After 7.2 mg of caffeic acid, 16 mg of HBTU, 8 mg of HOBT and 48 μL of DIEA were added, the mixture was stirred in a rotator for 3 h at room temperature. The resulting NPs were centrifuged (8500 rpm, 15 min) and washed with DMF several times.

II. 4 Preparation of PVP-coated Fe_3O_4 NPs

The mixture of 2.5 mL MC and 2.5 mL DMF was used as co-solvent for amphiphilic modification of Fe_3O_4 NPs. After 2.5 mg of oleate capped Fe_3O_4 NPs were dispersed in 5 mL of MC/DMF co-solvent, 120 mg of PVP (MW=10000) were added. The mixture was heated to 100 ℃ for 3 h. After cooling to room temperature, the resulting Fe_3O_4 NPs were poured dropwise into 10 mL of diethyl ether, centrifuged (4000 rpm, 5 min) and dispersed in ethanol.

II. 5 Preparation of magnetic silica NPs (M silica NPs)

Catechol functional group-modified silica NPs (1 mg) was dispersed in 5 mL PVP-coated Fe_3O_4 NPs (0.35 mg) was dispersed in 5 mL of ethanol. Then, the two solutions were mixed and sonicated for 1 h at room temperature. The resulting silica NPs were centrifuged (7000 rpm, 10 min) and washed with isopropyl alcohol for several times. To introduce the silica coated surface, the resulting NPs were dispersed in 5 mL of IPA. Then 50 μL of TEOS and 100 μL of ammonium hydroxide were added and stirred in a rotator for 18 h at room temperature. The resulting magnetic silica NPs (M silica NPs) were centrifuged (7000 rpm, 10 min) and washed with absolute ethanol several times.

II. 6 Preparation of magnetic silver nanoshell (M AgNS)

To introduce the thiol functional groups on the surface of M silica NPs, 1 mg of M silica NPs was dispersed in 1 mL of absolute ethanol. Then 10 μL of MPTS, 10 μL of H_20 and 50 μL of ammonium hydroxide were added and mixed in a shaking incubator (190 rpm) for 1 h at 50 ℃. The resulting M silica NPs were centrifuged and washed with absolute ethanol several times. To obtain silver (Ag) surface on M silica NPs, 0.2 mg of PVP (MW=40000) was dispersed in 1 mL of ethylene glycol (EG). 2.5 mg of silver nitrate ($AgNO_3$) was dissolved in 1 mL of EG. Then, thiol-functionalized M silica NPs (0.5 mg) was dispersed in 50 μL of absolute ethanol, and added to the PVP solution. After mixing, 1 mL of $AgNO_3$ solution to the mixture and 4 μL of octylamine was added to the mixture and mixed in a rotor for 1 h at room temperature. The resulting magnetic Ag nanoshell (M AgNS) was centrifuged (8500 rpm, 10 min) and washed with absolute ethanol several times.

II. 7 Detection processes of chemicals with M AgNS

Chemicals such as 4-FBT, thiram and malathion were detected with M AgNSs (0.5 mg) was dispersed in 900 μL of ethanol. Then, 100 μL of a test chemical was added to the M AgNS solution and mixed in a microtube mixer for 1 h at room temperature. The resulting M AgNS was centrifuged (13000 rpm, 5 min) and washed with ethanol several times for SERS detection.

II. 8 SERS measurement via M AgNS aggregation by an external magnet

A magnet was used (4000 gauss) for M AgNS aggregation. After a certain chemical was adsorbed on M AgNS, 20 μL of M AgNS was loaded on a slide glass and the magnet was placed underneath of the slide glass. After drying the M AgNS, SERS spectrum was obtained by a potable Raman system with 785 nm laser.

II. 9 The effect of Hot spots of M AgNSs on SERS Sensitivity

To study for the effect of 'hot spots' among M AgNSs, M AgNSs (1 mg/mL) which was treated with 10 mM of 4-FBT and M silica NPs (1 mg/mL) were prepared. M AgNSs (4-FBT treated) and M silica NPs were mixed and dispersed at the ratio of 1:1, 1:3, 1:7 and 1:15 in a micro tube. 4-FBT treated M AgNSs (20 μL) were loaded on a slide glass and was applied 4000 gauss magnet to induce NP's aggregates. The SERS spectrum of M Ag NSs [10 mM 4-FBT] (A) was obtained by a portable Raman system with 785 nm laser. The SERS spectra of 1:1 (B), 1:3 (C), 1:7 (D) and 1:15 (E) mixed solution were obtained in the same way.

III. Results and Discussion

III. 1 Preparation of M AgNSs

M AgNSs were synthesized as shown in Figure 3.1. Silica NPs were used due to their ease of functionalization and synthesis. First, uniform sized silica NPs (250 nm) were synthesized by Stöber method and functionalized with amine groups. Then the amine groups were converted to catechol groups onto the surface of silica NPs via amide bond formation between amine and caffeic acids. The Fe_3O_4 NPs obtained were stabilized in chloroform by oleic acid ligands. So, polyvinylpyrrolidone (PVP) was added in order to introduce hydrophilicity onto the surface of Fe_3O_4 NPs. Then, the PVP coated Fe_3O_4 NPs were added to the catechol functionalized silica NPs so that Fe_3O_4 NPs can be adsorbed on the surface of silica NPs via coordination bondings. Then, the surface of the resulting silica NPs were with silica affording M silica NPs. After the surface of M silica NPs was functionalized with thiol group, 7.3 mM of $AgNO_3$ was added with octylamine as a reducing agent.

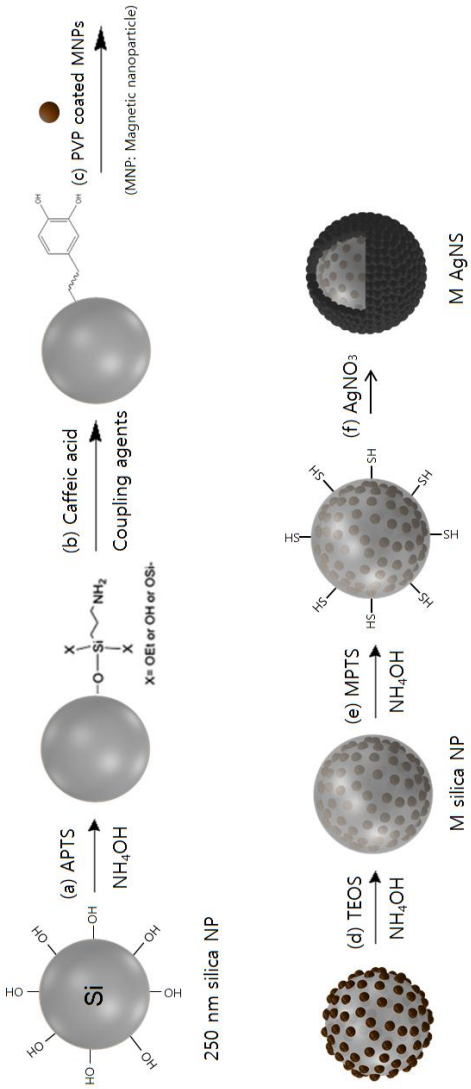

Figure 3.1 Schematic illustration of M AgNS synthesis.

(a) (3-aminopropyl)triethoxysilane (b) caffeic acid, HOBT, HBTU and *N,N*-diisopropylethylamine (c) PVP coated magnetic nanoparticles (d) Tetraethyl-orthosilicate (e) 3-mercaptopropyltrimethoxysilane (f) silver nitrate

III. 2 Characterization of M AgNSs

M AgNSs were characterized by transmission electron microscopy (TEM), scanning electron microscopy (SEM), UV/Vis spectrophotometer, and physical property measurement system (PPMS). Figure 3.2 shows the TEM images of each NP. Figure 3.2a shows silica NP with a diameter of 250 nm and 3.2b for Fe_3O_4 NPs embedded silica NP. The size of Fe_3O_4 NPs is about 25 nm, and they are uniformly distributed on the surface of silica NP. Figure 3.2c shows TEM images of M silica NP which has silica coated surface, Figure 3.2d for M AgNS shows TEM image, and Figure 3.2e for SEM image of M AgNS. As shown in Figure 3.2e, it was shown that M AgNS has a bumpy shaped Ag shell on the surface. This structure can create 'hot spots' that can induce a strong EM field enhancement compared to smooth surfaces. From Figure 3.2 images, it was proved that proper NPs were synthesized according to the each step. Figure 3.3.a. shows the absorbance spectra of M silica NPs and M AgNSs. Compared to the spectrum of M silica NPs, M AgNSs showed broad absorption band in NIR region due to its bumpy Ag shell structure. This broad absorption band in NIR can be beneficial when using a portable Raman system

with 785 nm laser. Figure 3.3b shows magnetic property of M AgNSs and the result of magnet induced aggregation. It shows the hysteresis loop of M AgNSs, which means that the M AgNSs had a superparamagnetism. This superparamagnetism properly gives a benefit to M AgNSs which can be dispersed in solution properly without leaving aggregated NPs. Below, the photo shows the magnetic property of M AgNS by the magnet application. From this, it was proved that the M AgNSs were easily aggregated by an external of magnet inducement in 5 mins.

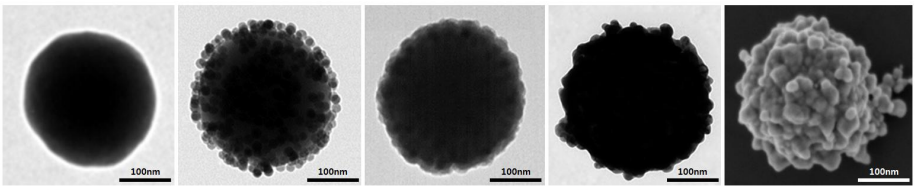

Figure 3.2 TEM images of, (a) 250 nm silica NP, (b) Fe_3O_4 embedded silica NP, (c) Magnetic silica NP, (d) Magnetic Ag nanoshell, and SEM image of (e) Magnetic Ag nanoshell

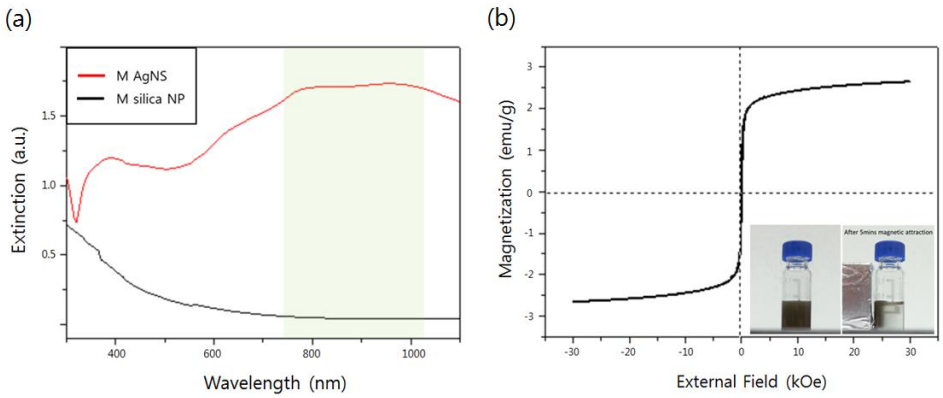

Figure 3.3 Characterization of M AgNSs. (a) UV/Vis extinction spectrums of M AgNS and M silica NP, (b) Hysteresis loop of M AgNSs and magnetic property of M AgNS by the magnet application.

III. 3 SERS spectra of 4-FBT on M AgNSs before and after aggregation by an external magnet

As shown in Figure 3.4, the SERS spectra of 4-FBT on M AgNSs were compared. 4-FBT (10 mM) was added M AgNSs (0.5 mg) in ethanol solution and mixed for 1 h at room temperature. To obtain the SERS spectrum in solution, 10 μg of M Ag NSs (treated with 4-FBT) were added in 100 μL of ethanol in a microtube. After the solution was put into the capillary tube, the SERS spectrum was obtained at 1075 cm^{-1} by a portable Raman system with 785 nm laser. In the same way, to obtain the SERS spectrum after aggregation, 10 μg of M AgNSs[4-FBT] were loaded on a slide glass and induced aggregated by a 4000 gauss magnet. After the aggregation, the SERS spectrum was obtained. As shown in Figure 3.4, before aggregation, the average SERS intensity at 10 mM of 4-FBT was about 1800, and 25220 after aggregation by magnet. The SERS intensity after aggregation by a magnet is about 14 times stronger than before aggregation. Through this result, it is expected that the aggregation by a magnet could lead to enhanced SERS signal.

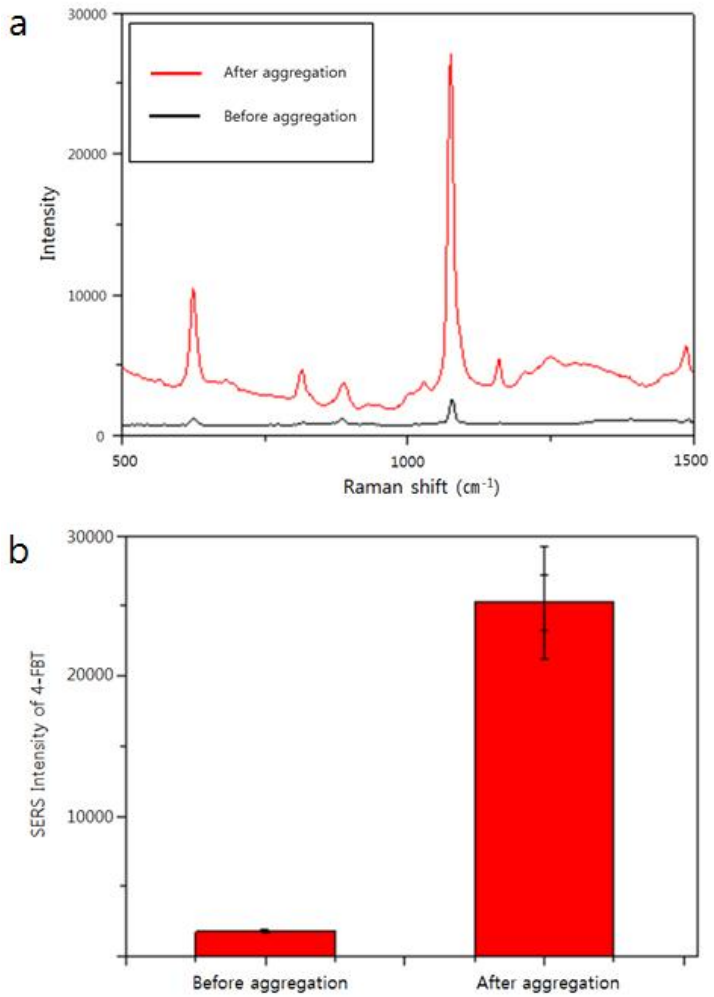

Figure 3.4 SERS spectra of 4-FBT on M AgNSs aggregation by a magnet (a) SERS spectra of 4-FBT on M AgNSs with the 785nm photo-excitation of 90 mW laser power and light acquisition of 1 s. (b) SERS intensity comparison between before and after aggregation at 1075 cm-1.

III. 4 SERS spectra of 4FBT at various concentrations with M AgNS

Figure 3.5 shows SERS spectra of 4-FBT at various concentrations of 10 mM, 1 mM, 100 μM, 10 μM and 1 μM on M AgNSs. 4-FBT was added to 0.5 mg of M AgNSs in ethanol solution and mixed for 1 h at room temperature. After washing, 10 μg of the resulting M AgNS [4-FBT] was loaded on a slide glass and induced aggregating by 4000 gauss magnet. The SERS signals were measured at 1075 cm^{-1}. Figure 3.5.a shows that the average SERS intensity at 10 mM of 4-FBT was about 25,250, and the intensity at 1 mM was about 22,760. Showing that the SERS intensities between the two cases were similar considered that there is a saturation concentration for 4-FBT on M AgNSs between 1 and 10 mM. On the other hand, the SERS intensity at 100 μM of 4-FBT was 15,440, 570 for 10 μM and 160 for 1 μM. From the Figure 3.6.b, it was shown that the SERS intensity increases according to the concentration of 4-FBT. In addition, the detection limit for 4-FBT was 1 μM, corresponding 16ppm.

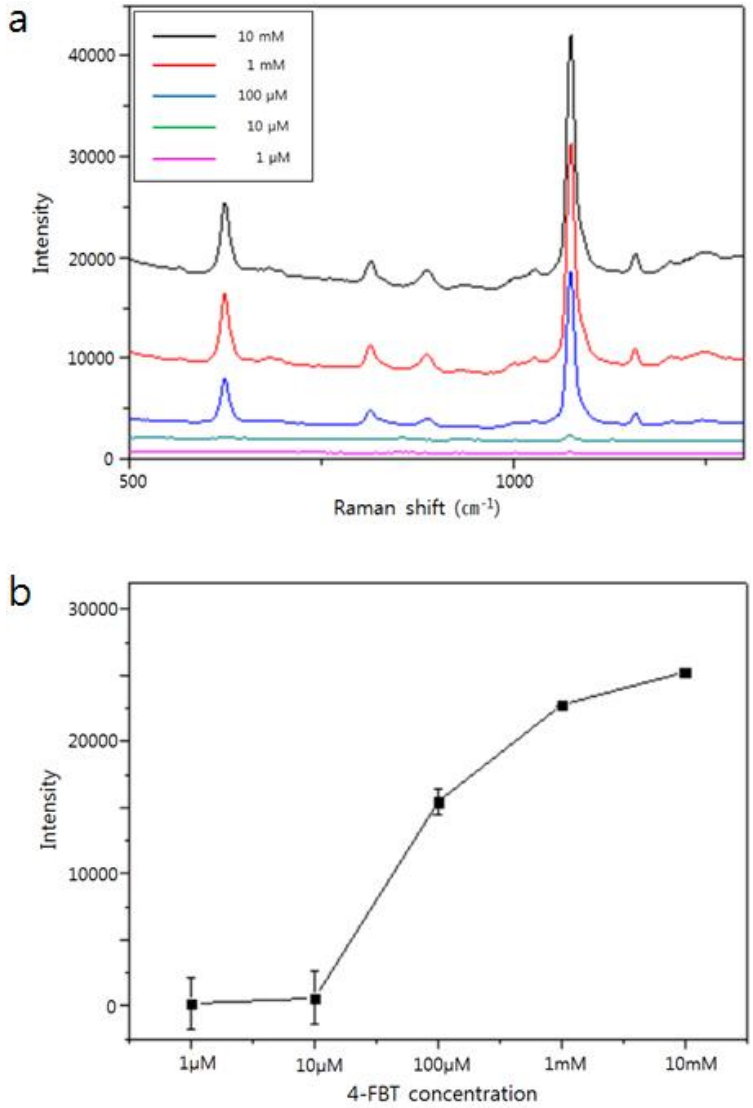

Figure 3.5 SERS spectra of 4FBT on M AgNS (a) SERS spectra of 4-FBT at various concentrations on M AgNSs with 785nm photo-excitation of 90 mW laser power and light acquisition of 1 s. (b) The SERS intensity of 4-FBT at 1075 cm^{-1} on M AgNSs.

III. 5 SERS measurement of thiram, malathion on M AgNSs

To confirm the detection capability of M AgNS for other chemicals, the SERS spectrum of thiram and malathion were measured by the same method. Thiram and malathion are widely used pesticides. Thiram has been used to prevent fungal disease in seed and crops and also used to prevent fruit trees from damage by animals such as rabbits and deer.[21] Malathion is generally used in agriculture, residential landscaping, and public recreation areas. In USA, it is the most commonly used insecticide. Each chemical was added to 0.5mg of M AgNSs in ethanol and mixed for 1 hour as before. Figure 3.6 shows the comparison graph of SERS signal for each chemical in solution state and after magnet induced aggregation. As shown in Figure 3.6.a, the SERS signals of thiram were measured at 560 cm^{-1}. The SERS intensity of thiram at 10 μM was about 2800 after aggregation by a magnet. Compared to them, the SERS intensity in solution state was much weaker than it. Likewise, the SERS signals of malathion were measured at 1580 cm^{-1}. The SERS intensity of malathion at 1 mM was about 1400 after aggregation by a magnet. Compared to them, the intensity in solution state was also

much weaker than it. From these results, it was considered that M AgNS has a capability to detect other kinds of chemicals as long as it contains functional group, chemicals can have affinity to metal surface. Furthermore, thess results were obtained was measured by a portable Raman spectrometer. This proves that M AgNS has a capability to detect the chemicals in on-site, immediately and rapidly.

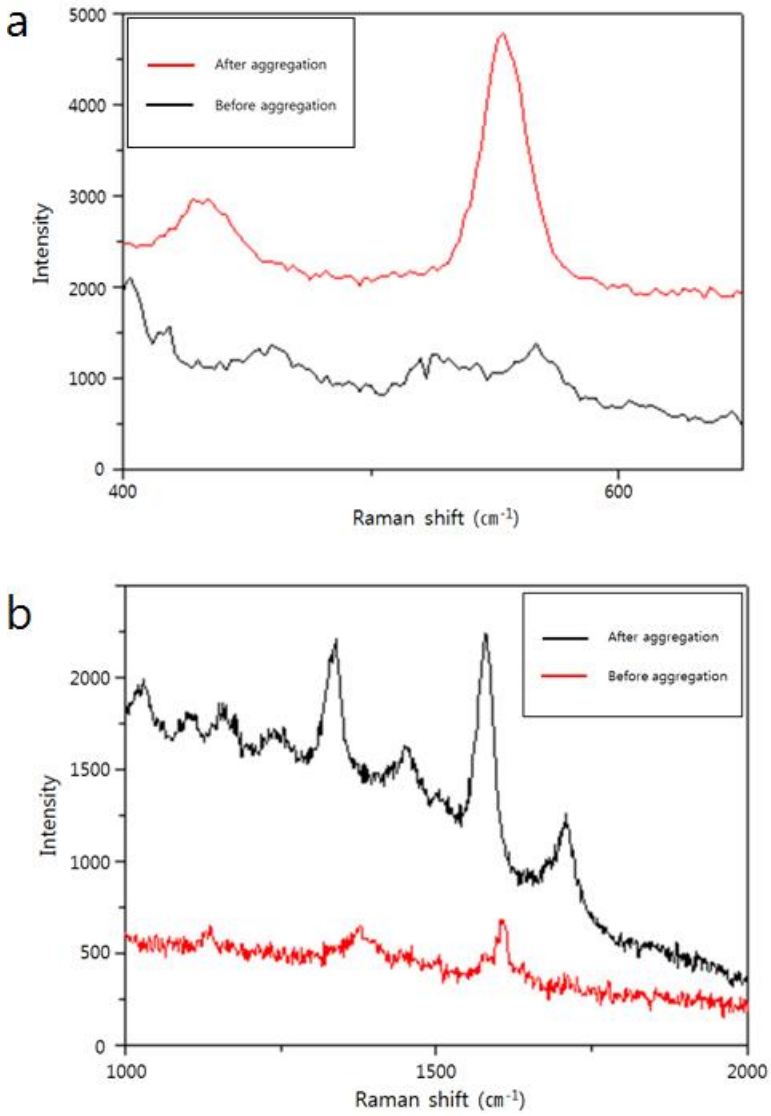

Figure 3.6. SERS measurement of thiram, malathion on M AgNSs with the 785nm photo-excitation of 60 mW laser power and light acquisition of 5 s (a) SERS spectra of 10 μM thiram on M AgNSs. (b) SERS spectra of 1 mM thiram.

III. 6 The effect of Hot spots of M AgNSs on SERS Sensitivity

To study the effect of 'hot spots' generated by M AgNSs on SERS sensitivity, several experiments using M silica NPs and M AgNSs were desinged. For this, we made assumptions as shown in Figure 3.7. If the SERS intensity from single M AgNS (4-FBT treated) particle is I_0, the intensity of the SERS peak from Fig 3.7.a would be also I_0, even after aggregation by an external magnet. In the same way, the intensity of the SERS peak from Fig 3.7.b is expected to be stronger than $3 \times I_0$, and that from Fig 3.7.c is also expected to be stronger than $9 \times I_0$ if the 'hot spots' are generated among the M AgNSs. Having these assumptions in mind, actual experiment was performed. First, M AgNS was treated with 4-FBT solution (10 mM), and dispersed in ethanol (1 mg/ mL). M silica NPs dispersion was also prepared in ethanol (1 mg/ mL). Then, M AgNSs (4-FBT treated) and M silica NPs were mixed according to the predetermined ratios. The SERS spectra of the solution at 1075 cm^{-1} were measured after aggregation. As shown in Table 1, the relative SERS intensities were obtained according to the ratio of M

AgNSs. Figure 3.8. shows the expected and the measured SERS intenties. If there are enough ‘hot spots’ generated among M AgNS, the slope of measured intensity graph should appear upper than the standard one. However, the slope of measured intensity graph was under the standard one. From these results, we proved that ‘hot spot’ effect was much weaker than expected.

In addition, SEM images of M AgNSs after aggregation by an external magnet were obtained as shown in Figure 3.9. From the Figure, it was shown that the distance of each M AgNS was not close enough to form the hot spots. However, M AgNss rather formed multi-layered stacked structure when aggregated by a magnet. This multi-layered structure enables laser light to be reached to the bottom part of the M AgNSs layer and enhance the SERS signals. Through this aggregation experimetn by a magnet, we can conclude that the increase of the SERS intensity maily comes from the multi-layered structure of M AgNSs, not form the ‘hot spot’ formation among M AgNSs.

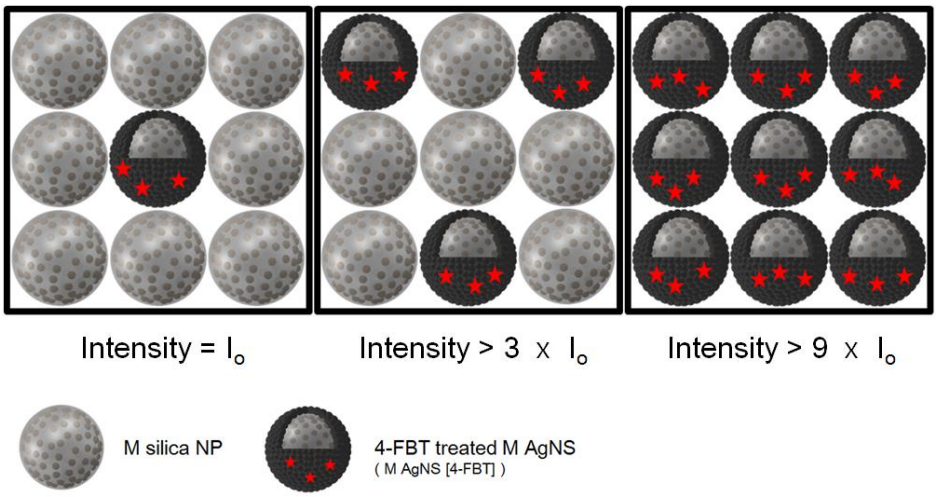

Figure 3.7 Illustration of expected SERS intensity of M AgNSs when aggregated by a magnet.

Table 1. Relative SERS Intensities of Mixture of M AgNSs and M Silica NPs after Aggregation by a Manget [a].

M AgNSs x 100 / (M AgNSs + M silica NPs)	Relative Intensity
100 %	5.7
50 %	3.1
25 %	2.6
12.5 %	1.9
6.25 %	1

a. Peak intensity at 1075 cm^{-1} was measured and normalized by the value from 6.25 %.

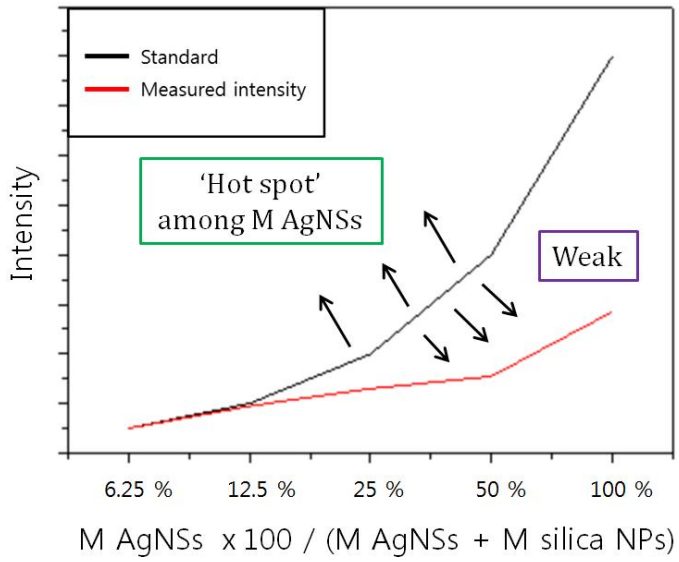

Figure 3.8 Expected and measured SERS intenty graph accoding to the ratio of M AgNSs.

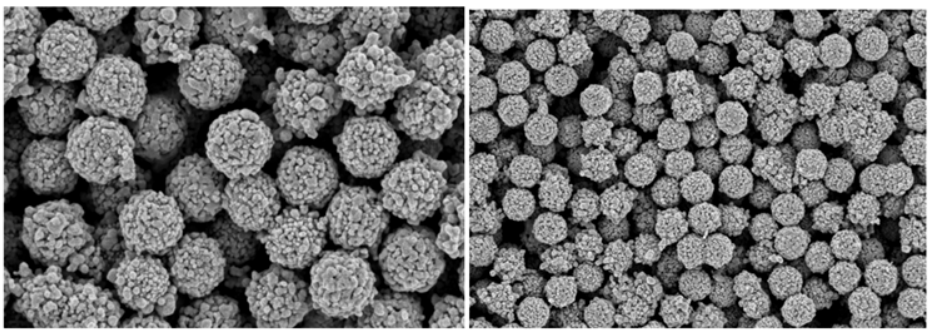

Figure 3.9 Multi-layered stacked structure of M AgNSs after aggregation by a magnet

IV. Conclusion

Magnetic silver nanoshell (M AgNS) was synthesized which has Fe_3O_4 NPs at the core part, and bumpy shaped Ag shell at the outer part of silica nanoparticles. Various concentrations of 4-FBT were added to the M AgNS, and SERS peak at 1075 cm^{-1} can be detected as low as 1 μM of 4-FBT after magnet induced M AgNS aggregation. It was also shown that when the concentrations of 4-FBT increased, the SERS intensities also enhanced accordingly.

The main factors for the enhanced SERS intensity comes from the bumpy shaped Ag surface structure and the increased number of M AgNSs by the magnet aggregation within a focal diameter of the Raman spectrometer laser. On the other hand, the effect of 'hot spot' formation among M AgNSs was weaker than expectation. It was also considered that M AgNS forms the multi layered stacked structure when aggregated by a magnet, which has a positive effect on the enhanced SERS signal.

M AgNS is a sensitive nanoprobe which can detect Raman chemical molecules at low concentration, and can be used for on site detection of pesticides such as thiram and malathion by portable Raman system.

V. References

1. Lane, L. A.; Qian, X.; Nie, S., SERS nanoparticles in medicine: from label-free detection to spectroscopic tagging. *Chemical reviews* **2015,** *115* (19), 10489-10529.

2. Jun, B. H.; Noh, M. S.; Kim, J.; Kim, G.; Kang, H.; Kim, M. S.; Seo, Y. T.; Baek, J.; Kim, J. H.; Park, J., Multifunctional Silver-Embedded Magnetic Nanoparticles as SERS Nanoprobes and Their Applications. *Small* **2010,** *6* (1), 119-125.

3. Sharma, B.; Cardinal, M. F.; Kleinman, S. L.; Greeneltch, N. G.; Frontiera, R. R.; Blaber, M. G.; Schatz, G. C.; Van Duyne, R. P., High-performance SERS substrates: Advances and challenges. *MRS bulletin* **2013,** *38* (08), 615-624.

4. Wang, Y.; Wei, H.; Li, B.; Ren, W.; Guo, S.; Dong, S.; Wang, E., SERS opens a new way in aptasensor for protein recognition with high sensitivity and selectivity. *Chemical Communications* **2007,** (48), 5220-5222.

5. Polavarapu, L.; Xu, Q.-H., Water-soluble conjugated polymer-induced self-assembly of gold nanoparticles and its application to SERS. *Langmuir* **2008,** *24* (19), 10608-10611.

6. Kubackova, J.; Fabriciova, G.; Miskovsky, P.; Jancura, D.; Sanchez-Cortes, S., Sensitive surface-enhanced raman spectroscopy (SERS) detection of organochlorine pesticides by alkyl dithiol-functionalized metal nanoparticles-induced plasmonic hot spots. *Analytical chemistry* **2014,** *87* (1), 663-669.

7. Alvarez-Puebla, R. A.; Liz-Marzán, L. M., SERS-based diagnosis and biodetection. *Small* **2010,** *6* (5), 604-610.

8. Vo-Dinh, T.; Wang, H. N.; Scaffidi, J., Plasmonic nanoprobes for SERS biosensing and bioimaging. *Journal of biophotonics* **2010,** *3* (1-2), 89-102.

9. Le Ru, E.; Meyer, M.; Blackie, E.; Etchegoin, P., Advanced aspects of electromagnetic SERS enhancement factors at a hot spot. *Journal of Raman Spectroscopy* **2008,** *39* (9), 1127-1134.

10. Yang, J.-K.; Kang, H.; Lee, H.; Jo, A.; Jeong, S.; Jeon, S.-J.; Kim, H.-I.; Lee, H.-Y.; Jeong, D. H.; Kim, J.-H., Single-step and rapid growth of silver nanoshells as SERS-active nanostructures for label-free detection of pesticides. *ACS applied materials & interfaces* **2014,** *6* (15), 12541-12549.

11. Farcau, C.; Astilean, S., Mapping the SERS efficiency and hot-spots localization on gold film over nanospheres substrates. *The Journal of Physical Chemistry C* **2010,** *114* (27), 11717-11722.

12. Shanmukh, S.; Jones, L.; Driskell, J.; Zhao, Y.; Dluhy, R.; Tripp, R. A., Rapid and sensitive detection of respiratory virus molecular signatures using a silver nanorod array SERS substrate. *Nano letters* **2006,** *6* (11), 2630-2636.

13. Ciou, S.-H.; Cao, Y.-W.; Huang, H.-C.; Su, D.-Y.; Huang, C.-L., SERS enhancement factors studies of silver nanoprism and spherical nanoparticle colloids in the presence of bromide ions. *The Journal of Physical Chemistry C* **2009,** *113* (22), 9520-9525.

14. Schütz, M.; Steinigeweg, D.; Salehi, M.; Kömpe, K.; Schlücker, S., Hydrophilically stabilized gold nanostars as SERS labels for tissue imaging of the tumor suppressor p63 by immuno-SERS microscopy. *Chemical Communications* **2011,** *47* (14), 4216-4218.

15. Yoon, I.; Kang, T.; Choi, W.; Kim, J.; Yoo, Y.; Joo, S.-W.; Park, Q.-H.; Ihee, H.; Kim, B., Single nanowire on a film as an efficient SERS-active platform. *Journal of the American Chemical Society* **2008,** *131* (2), 758-762.

16. McLellan, J. M.; Li, Z.-Y.; Siekkinen, A. R.; Xia, Y., The SERS activity of a supported Ag nanocube strongly depends on its orientation relative to laser polarization. *Nano letters* **2007,** *7* (4), 1013-1017.

17. Shiohara, A.; Wang, Y.; Liz-Marzan, L. M., Recent approaches toward creation of hot spots for SERS detection. *Journal of Photochemistry and Photobiology C: Photochemistry Reviews* **2014,** *21*, 2-25.

18. Yang, L.; Li, P.; Liu, H.; Tang, X.; Liu, J., A dynamic surface enhanced Raman spectroscopy method for ultra-sensitive detection: from the wet state to the dry state. *Chemical Society Reviews* **2015,** *44* (10), 2837-2848.

19. Eshkeiti, A.; Narakathu, B. B.; Reddy, A.; Moorthi, A.; Atashbar, M.; Rebrosova, E.; Rebros, M.; Joyce, M., Detection of heavy metal compounds using a novel inkjet printed surface enhanced Raman spectroscopy (SERS) substrate. *Sensors and Actuators B: Chemical* **2012,** *171*, 705-711.

20. Tripp, R. A.; Dluhy, R. A.; Zhao, Y., Novel nanostructures for SERS biosensing. *Nano Today* **2008,** *3* (3), 31-37.

21. Li, D.-W.; Zhai, W.-L.; Li, Y.-T.; Long, Y.-T., Recent progress in surface enhanced Raman spectroscopy for the detection of environmental pollutants. *Microchimica Acta* **2014,** *181* (1-2), 23-43.

Abstract in Korean

표면증강 라만 산란 (SERS)은 금이나 은과 같은 귀금속 나노 프로브 표면에 분자 물질이 흡착되었을 때, 라만 산란 신호가 증가하는 현상을 말한다. 이것은 좁은 간격의 스펙트럼을 갖고, 지문과 같이 물질마다의 고유한 패턴이 있는 특성이 있다. 또한 신호가 민감하고 광퇴색 현상에도 안정적이기 때문에 다양한 종류의 물질을 분석하는데 효과적인 기술로서 사용되고 있다. 강한 SERS 신호를 얻기 위해서는 금속 나노 프로브의 구조가 매우 중요하기 때문에 낮은 농도에서도 물질을 검출할 수 있는 민감한 프로브를 개발하는 연구가 활발하게 진행되고 있다. 본 연구에서는 새로운 종류의 SERS 나노 프로브로서 250 nm 크기의 실리카 나노 입자를 기반으로 속에는 자석 나노 입자를 포함하고 겉에는 울퉁불퉁한 모양의 은 표면을 갖는 자석 은 나노 쉘을 개발하였다. 은 표면의 구조는 울퉁불퉁한 모양으로서 이를 통해 '핫 스팟'을 형성하여 더 강한 SERS 신호를 도출할 수 있었다. 또한 SERS 신호 세기는 자석을 통한 뭉침 현상으로 인하여 더 증가될 수 있었고 자석 은 나노 쉘을 이용하여 4-fluorothiophenol 을 1 μM 의 낮은 농도까지 검출할 수 있었다.

또한 농장에서 주로 사용되는 살충제의 일종인 thiram 과 malathion 도 자석 은 나노쉘을 이용하여 낮은 농도에서 검출할 수 있었다. Thiram 의 경우 한계 검출 농도는 10 uM 이었고, 이것은 3 ppm 이다. 본 연구를 통해 훗날 자석 은 나노 쉘을 이용하여 휴대용 라만 분광기로 현장에서 즉시, 단시간 내로 원하는 분석 물질을 검출할 수 있다고 기대된다.

학 번 : 2015-21063